

# Water waves over a random bottom

W. CRAIG<sup>1</sup>†, P. GUYENNE<sup>2</sup> AND C. SULEM<sup>3</sup>

<sup>1</sup>Department of Mathematics, McMaster University, Hamilton, ON L8S 4K1, Canada

<sup>2</sup>Department of Mathematical Sciences, University of Delaware, Newark DE 19716, USA

<sup>3</sup>Department of Mathematics, University of Toronto, Toronto, ON M5S 3G3, Canada

(Received 1 August 2008; revised 16 July 2009; accepted 16 July 2009)

This paper gives a new derivation and an analysis of long-wave model equations for the dynamics of the free surface of a body of water which has random bathymetry. This is a problem of hydrodynamical significance to coastal regions and to global-scale propagation of tsunamis, for which there may be imperfect knowledge of the detailed topography of the bottom. The surface motion is assumed to be in a long-wavelength dynamical regime, while the bottom of the fluid region is given by a stationary random process whose realizations vary over short length scales and are decorrelated on the longer principal length scale of the surface waves. Our basic conclusions are that coherent solutions propagating over a random bottom maintain basic properties of their structure over long distances, but however, the effect of the random bottom introduces uncertainty in the location of the solution profile and modifies the amplitude by random factors. It also gives rise to a random scattered component of the solution, but this does not result in the dispersion of the principal component of the solution, at least over length and time scales considered in this regime. We illustrate these results with numerical simulations.

The mathematical question is one of homogenization theory in the long-wave scaling regime, for which our work is a reappraisal of the paper of Rosales & Papanicolaou (*Stud. Appl. Math.*, vol. 68, 1983, pp. 89–102). In particular, we derive appropriate Boussinesq and Korteweg–deVries type equations with random coefficients which describe the free-surface evolution in this regime. The derivation is performed from the point of view of perturbation theory for Hamiltonian partial differential equations with a small parameter, with a subsequent analysis of the random effects in the resulting solutions. In the analysis, we highlight the distinction between the effective equations for a fixed typical realization, for which there are coherent solitary-wave solutions, and their ensemble average, which may exhibit diffusive effects. Our results extend the prior analysis to the case of non-zero variance  $\sigma_\beta^2 > 0$ , and furthermore the analysis identifies the canonical limit random process as a white noise with covariance  $\sigma_\beta^2 \delta(X - X')$  and quantifies the variations in phase and amplitude of the principal and scattered components of solutions. We find that the random topography can give rise to an additional linear term in the KdV limit equations, which depends upon a skew property of the random process and whose sign affects the stability of solutions. Finally we generalize this analysis to the case in which the bottom has large-scale deterministic variations on which are superposed random fluctuations with slowly varying statistical properties.

---

† Email address for correspondence: craig@math.mcmaster.ca

## 1. Introduction

This paper gives a systematic derivation and analysis of the equations of motion of water waves in the free surface of a channel of fluid lying over a variable bottom. It is well known that in a channel of fixed constant depth, the Euler equations for an incompressible irrotational flow have solitary-wave solutions, which propagate momentum and energy rapidly over long distances with no attenuation. The question is to what extent this capability is retained when the fluid is not of constant depth, in which case approximately coherent wave motions will propagate through regions of fluid with varying depth, and significant modulation and wave scattering may take place. It is assumed that the detailed variations of the bottom are known only imperfectly, so that over short spatial scales they are modelled by a stationary process  $\beta(x; \omega)$  of given statistics, which exhibit properties of decorrelation under spatial translations. The correlation length of the short-scale bottom variations is of the same order as the depth. The typical wavelength of a surface deformation is taken to be long with respect to this correlation length. The hydrodynamical significance of this work is to nonlinear wave propagation in coastal regions and to the hydrodynamics of tsunamis in mid-ocean, where variations of the bathymetry of the fluid region influence the dynamics of surface waves; however the details of the variations are approximately but not precisely known.

The main result of this paper is that nonlinear waves propagate as coherent structures in a fluid basin with a random bottom, but they are influenced by its statistical properties as well as individual realizations of the bathymetry and therefore have a degree of unpredictability. In particular, solutions are not significantly dispersed by random scattering, at least in the space–time regime that we consider. The influence of the bathymetry includes (i) a random phase affecting the location of the solution (similar to the findings of Rosales & Papanicolaou 1983), (ii) a perturbation of the amplitude of the solution by a random factor and (iii) a random scattered component. We quantify all of these effects and show that in the long-wave limit, the perturbations to the phase are asymptotic to Brownian motion, while the perturbations to the amplitude and scattering are asymptotic to white noise processes.

Our point of approach to this problem is through a formulation in terms of a perturbation theory for Hamiltonian partial differential equations (PDEs) and through the method of averaging of Hamiltonians and transformation theory introduced in Craig, Guyenne & Kalisch (2005). We derive in this systematic manner an appropriate form of a Boussinesq equation and from this a version of the Korteweg–deVries (KdV) equation which describe the propagation of long waves in the fluid surface over the rapidly varying bottom. This is a problem in homogenization theory, determining to what extent the free-surface motion can be described by a PDE with deterministic ‘effective’ coefficients or in contrast the extent to which ‘random, realization-dependent’ effects are retained in the solution.

Our work is a reappraisal by a different method of the results of Rosales & Papanicolaou (1983), who considered the same KdV scaling regime, in which two cases are studied: (i) a periodically varying bottom and (ii) a random bottom. The case in which the bottom varies periodically is shown in Rosales & Papanicolaou (1983) to homogenize fully, a result which is recovered in Craig *et al.* (2005). The fact that the periodic case homogenizes to all orders can be seen in the scale separation lemma of the latter reference.

In the present work we take up the case of a randomly varying bottom, for which the bathymetry is modelled as realizations of a stationary ergodic process which exhibits

sufficiently strong properties of mixing; this quantifies the decorrelation of the statistics of realizations of a random topography. As in Rosales & Papanicolaou (1983) we show that this problem does not homogenize fully and that it retains realization-dependent effects which are as significant as the dispersion and the nonlinearity in the long-wave limit. These random terms are retained in the basic Hamiltonian PDE for the evolution of surface waves.

The result is that for each individual realization, the equation with random coefficients retains the property of possessing coherent solutions which propagate mass and energy with little loss. We furthermore quantify the effects of random modulation of solutions and random scattering that do occur. In particular, we find that coherent solutions retain the signature of the random bottom in two ways. First, they propagate in characteristic coordinates which are themselves random, given by a Brownian motion, so that asymptotically, phase variations are Gaussian distributed. Second, the amplitude of coherent solutions is subject to random modulation, given by a white noise process which is correlated with the phase variations. Finally, there is an effect of random scattering given again by a superposition of canonical processes. Our analysis applies to the case in which the variance  $\sigma_\beta^2$  of the random process  $\beta(x; \omega)$  is non-vanishing, which was left open in the treatment given in Rosales & Papanicolaou (1983). A proof of this result and the characterization of the limit processes is through Donsker's invariance principle, with one determining parameter being the variance  $\sigma_\beta^2$ . Related work on corrections to homogenization theory and generalized central limit theorems appears in Bal (2008).

While the model equations for each realization of the random process come from Hamiltonian PDEs, and therefore are related to conservative evolution equations, their ensemble average is not. In addition to giving distinct expressions for solutions and for their ensemble averages, we derive nonlinear dissipative evolution equations for averages of the quantities of physical interest, which again reflect the canonical nature of the limit process that is encountered in this problem. These equations are closely related to the KdV equation modified with a dissipation term that was derived in Mei & Li (2004) in a perturbation theory for the ensemble average of water waves over a random rough seabed. However in the regime we investigate, the dissipation is of higher order and does not influence solutions at the level of the nonlinear and dispersive effects.

As an extension of our approach, we generalize the long-wave perturbation analysis to the situation in which the topography of the bottom varies deterministically over spatial scales of the order of the typical wavelength, while at the same time there are random short-scale variations whose statistics are also allowed to vary on a long length scale. In this case the coefficients of the resulting KdV equation have both deterministic long-spatial-scale dependence and variations retained from the random effects, and the scattering due to the bottom variations depends upon both. This is probably the most realistic situation under consideration.

The results of our asymptotic analysis are illustrated by several numerical simulations of nonlinear wave propagation over random bathymetry. The evolution of solutions of our model equations are computed, given various realizations of the bottom topography. The effect of individual realizations of the bottom is seen in these simulations, as well as the effect of the overall statistics. In particular, the crest and centre of mass, relative to constant velocity trajectories, are perturbed by displacements consistent with the character of Brownian motion, while the amplitude perturbations and the scattered component are rougher and consistent with white noise.

There is a large physics and mathematics literature on the problem of wave propagation in random media, principally focusing on the phenomenon of localization for solutions of linear equations (Anderson localization in the context of the Schrödinger operator). In the linear regime, the analogy between free-surface dynamics and Anderson localization was pointed out in Devillard & Souillard (1986), Devillard, Dunlop & Souillard (1988) and Nachbin (1995), after which the analysis of this idea was pursued in a series of papers, which includes the papers of Fouque, Garnier & Nachbin (2004) and Nachbin & Sølna (2003) on the diffusion of the ensemble averages of solutions of the linear approximation to the shallow-water theory over random topography. Experimental support for the idea that water waves over a randomized bed are localized due to random-scattering effects has been reported in Belzons, Guazzelli & Parodi (1988).

Our work concerns the nonlinear problem of surface water waves over a random variable bottom and the associated long-wave and modulational asymptotic limits. The earlier analyses are by Howe (1971) and Rosales & Papanicolaou (1983) which we have cited above. Much more recent contributions include the series of papers by Mei & Hancock (2003) and Grataloup & Mei (2003) on the modulational scaling regime and by Pihl, Mei & Hancock (2002) on its extensions to the three-dimensional case. This work focuses on the temporal behaviour of the ensemble averages of solutions, and the result is that they satisfy a nonlinear Schrödinger equation with an additional dissipative term. The analogue of this picture of theirs in the long-wave scaling regime appears in Mei & Li (2004), in which, starting from a Boussinesq approximation, they derive that the ensemble averages satisfy a KdV equation with an additional linear dissipative term. In related work, Ardhuin & Herbers (2002) derived an energy balance equation for Bragg scattering of quasi-monochromatic waves by random topography, the variations of which are assumed to occur on scales of the order of the surface wavelength. The paper of Nakoulima *et al.* (2005) investigated the problem of soliton propagation over random topography, modelling the evolution directly with a dissipative KdV equation. In this analysis the bottom variations are assumed to be long compared to the soliton width, as opposed to the case in the present paper. Much closer to the situation that we consider, Garnier, Muñoz Grajales & Nachbin (2007) modelled the problem of long waves over short-length-scale random topography with a version of a Boussinesq equation, from which they derived an effective, dissipative KdV-like equation for the principal component of the solution. In the above work, the averaged quantities are shown to attenuate in time, with a slower rate than that predicted from the linear theory of a random sea bed. This is consistent with our own findings, while on the other hand, we show that for any particular realization of the bottom topography, solutions may have a well-defined solitary-wave component which represents a permanent, non-attenuating waveform. We also quantify the next-order corrections, which appear in the form of a random (white noise) amplitude modulation and a scattered wave. Since in nature we are presented with a given, albeit unknown, bottom, it is important to make the distinction between the behaviour of the solution for a fixed realization and the expected value of the solution which is the result of averaging over the ensemble of realizations. This is the point of view which we retain throughout the present paper.

The organization of the paper is as follows: §2 gives the problem of water waves in its Hamiltonian form, describes the long-wave scaling regime in the presence of short-scale variations of bathymetry and derives the model equations. The description of random topography given by stationary processes is in §3, along with the main theorem on scale separation. Using this information about limit processes, random

characteristic coordinates are introduced, with which we express solutions of the model equations and their limits. These solutions are random and are realization dependent. In §4, we discuss the ensemble average of solutions, a deterministic quantity which is a common focus of study. Section 5 gives an extension of our analysis to the more complicated case of random topography for which there are both large-scale deterministic variations and small-scale random fluctuations. In §6, we present numerical simulations of the long-wave model problem with random coefficients. Concluding remarks are given in §7.

## 2. Derivation of the asymptotic equations

The point of departure is the oceanographers' approximation to the Euler equations, namely a potential flow with Neumann boundary conditions on fixed surfaces and two nonlinear free-boundary conditions on the dynamic free surface. Following Zakharov (1968), we pose these equations as a Hamiltonian system. Using the approach in Craig *et al.* (2005), a long-wave analysis is performed in the context of Hamiltonian perturbation theory. To leading order, the solution decomposes into a principally right-moving component and a secondary left-moving one which satisfy a system of coupled equations with random coefficients. These are then solved in random characteristic coordinates, and the solution is shown to be consistent with the degree of approximation of the original equations.

### 2.1. Hamiltonian formulation and the long-wave regime

The fluid velocity is given in Eulerian coordinates by

$$v = \nabla\varphi, \quad \Delta\varphi = 0, \quad (2.1)$$

in the fluid domain  $S(\beta, \eta) = \{(x, y) \in \mathbb{R}^{n-1} \times \mathbb{R} : -h + \beta(x) < y < \eta(x, t)\}$ , where  $\varphi(x, y, t)$  is the velocity potential. The bottom-boundary condition is

$$\nabla\varphi \cdot N(\beta) = 0 \quad \text{at} \quad y = -h + \beta(x), \quad (2.2)$$

where  $N(\beta) = (1 + |\partial_x\beta|^2)^{-1/2}(\partial_x\beta, -1)$  is the exterior unit normal. The top boundary satisfies the usual kinematic and Bernoulli conditions

$$\left. \begin{aligned} \partial_t\eta &= \partial_y\varphi - \partial_x\eta \cdot \partial_x\varphi, \\ \partial_t\varphi &= -g\eta - \frac{1}{2}|\nabla\varphi|^2 \end{aligned} \right\} \quad \text{at} \quad y = \eta(x, t). \quad (2.3)$$

Here  $\beta(x)$  denotes the bottom deformation relative to a constant reference depth  $h$ , while  $\eta(x, t)$  denotes the surface elevation about the quiescent water level  $y=0$  and  $g$  is the acceleration due to gravity. A sketch of the situation is given in figure 1. This system can be written in Hamiltonian form

$$\partial_t\eta = \delta_\xi H, \quad \partial_t\xi = -\delta_\eta H, \quad (2.4)$$

with Hamiltonian functional given by the expression for the total energy

$$\begin{aligned} H &= \int \int_{-h+\beta(x)}^{\eta(x)} \frac{1}{2} |\nabla\varphi(x, y)|^2 dy dx + \int \frac{g}{2} \eta^2(x) dx \\ &= \frac{1}{2} \int \xi(x) G(\beta, \eta) \xi(x) + g\eta^2(x) dx, \end{aligned} \quad (2.5)$$

where  $\xi(x) = \varphi(x, \eta(x))$  gives the boundary values of the potential  $\varphi$  on the free surface. For simplicity of notation, the dependence of  $\eta$  and  $\xi$  on  $t$  has been dropped.

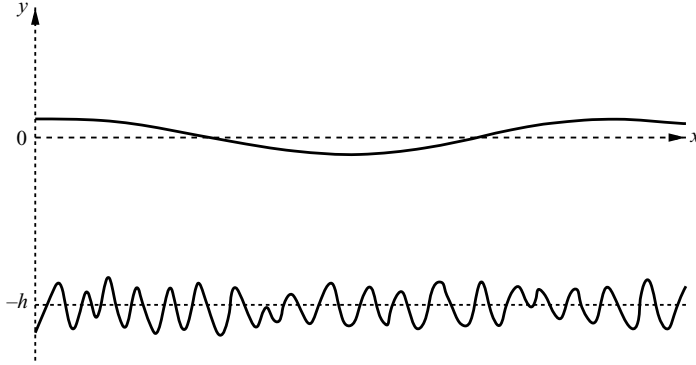


FIGURE 1. A sketch of long waves over a fluid domain with a random bottom.

In this form, the Dirichlet–Neumann operator  $G(\beta, \eta)$  expresses the normal derivative of the velocity potential on the free surface,

$$G(\beta, \eta)\xi(x) = \nabla\varphi(x, \eta(x)) \cdot N(\eta)(1 + |\partial_x\eta|^2)^{1/2}, \quad (2.6)$$

as a function of the boundary values  $\xi(x)$ , where  $N(\eta)$  is the exterior unit normal on the free surface. The Dirichlet–Neumann operator depends as well on the bottom topography given by  $y = -h + \beta(x)$ , as the velocity potential satisfies (2.2).

Define  $u := \partial_x\xi$  and rewrite (2.4) in terms of the variables  $(\eta, u)$ , giving

$$\partial_t \begin{pmatrix} \eta \\ u \end{pmatrix} = \begin{pmatrix} 0 & -\partial_x \\ -\partial_x & 0 \end{pmatrix} \begin{pmatrix} \delta_\eta H \\ \delta_u H \end{pmatrix}, \quad (2.7)$$

where

$$H = \frac{1}{2} \int u M(\beta, \eta) u + g\eta^2(x) dx, \quad (2.8)$$

with  $D_x M(\eta, \beta) D_x = G(\eta, \beta)$ .

We now seek solutions which depend principally upon the large-scale spatial variables  $X$  while depending upon  $x = X/\varepsilon$  at higher order in  $\varepsilon$ . With respect to the large spatial scale of the problem, the bottom topography varies rapidly, namely  $\beta(x) = \varepsilon\tilde{\beta}(X/\varepsilon)$ , and solutions appear in the form  $(\eta, u) = (\eta(X, t; \varepsilon), u(X, t; \varepsilon))$ .

We restrict our attention in the present paper to the case of dimension  $n = 2$ . In rescaled variables, the classical long-wave scaling

$$X = \varepsilon x, \quad u(x) = \varepsilon^2 \tilde{u}_\varepsilon(X) \quad \eta(x) = \varepsilon^2 \tilde{\eta}_\varepsilon(X), \quad (2.9)$$

puts us into the asymptotic regime of interest, for

$$\varepsilon^2 = \left(\frac{h}{\lambda}\right)^2 = \frac{a}{h} \ll 1, \quad (2.10)$$

where  $a$  and  $\lambda$  are the typical wave amplitude and wavelength, respectively. Solutions are then observed only at the larger scales, which is to say that one measures

$$\int f(X)(\eta_\varepsilon(X, t), u_\varepsilon(X, t)) dX \quad (2.11)$$

for test functions  $f \in \mathcal{S}(\mathbb{R})$ . The leading terms in  $\varepsilon$  of the evolution equations are selected by the asymptotic behaviour of the quantities

$$\int f(X) \begin{pmatrix} 0 & -\partial_X \\ -\partial_X & 0 \end{pmatrix} \begin{pmatrix} \delta_\eta H \\ \delta_u H \end{pmatrix} dX = \sum_{l=0}^L \varepsilon^l \int f(X) V^{(l)}(\eta_\varepsilon, u_\varepsilon) dX + o(\varepsilon^L). \quad (2.12)$$

Making the identification of this series to  $O(\varepsilon^L)$  with the effective approximate equations, we arrive at the expression

$$\partial_t \begin{pmatrix} \eta_\varepsilon \\ u_\varepsilon \end{pmatrix} = \sum_{l=0}^L \varepsilon^l V^{(l)}(\eta_\varepsilon, u_\varepsilon). \quad (2.13)$$

The asymptotic expansion and truncation of (2.12) may not necessarily retain Hamiltonian form, but they do describe the large-scale behaviour of (2.4). The main task in evaluating (2.12) for the water wave problem consists in expanding the Dirichlet–Neumann operator  $G$  in powers of the small parameter  $\varepsilon$ . The reader is referred to Craig *et al.* (2005) for details on the Taylor expansion of  $G$  in terms of  $\beta$  and  $\eta$ . The problem evidently has two spatial scales, for which we denote  $D_X = -i\partial_X$  and  $D_x = -i\partial_x$ . Using this notation, the operator whose action in the Fourier transform variables dual to  $x$  is given by multiplication by  $k \tanh(hk)$  is conveniently denoted by  $D_x \tanh(hD_x)$ .

Adopting the Ansatz that

$$u_\varepsilon = u_0(X, t) + \varepsilon u_1(X, t; \varepsilon), \quad (2.14)$$

$$\eta_\varepsilon = \eta_0(X, t) + \varepsilon \eta_1(X, t; \varepsilon) \quad (2.15)$$

the rescaled vector field calculated at  $O(\varepsilon^2)$  is

$$V_1 = -\partial_X \left[ h_\varepsilon(X) u_\varepsilon + \varepsilon^2 \eta_\varepsilon u_\varepsilon + \frac{h^3 \varepsilon^2}{3} \partial_X^2 u_\varepsilon \right], \quad (2.16)$$

$$V_2 = -\partial_X \left( g \eta_\varepsilon + \frac{\varepsilon^2}{2} u_\varepsilon^2 \right), \quad (2.17)$$

where criterion (2.12) is used. The corrected depth is

$$h_\varepsilon(X) = h - \varepsilon \gamma(X/\varepsilon) - \varepsilon^2 a_\beta, \quad (2.18)$$

where  $\gamma(x) := \operatorname{sech}(hD_x)\beta(x)$  and  $a_\beta := \mathbf{E}(\beta D_x \tanh(hD_x)\beta)$ . We use the notation  $\mathbf{E}(\mu)$  for the expected value of a random variable  $\mu$  with respect to the underlying probability measure  $\mathbf{P}$ . The presence of the smoothing operator  $\operatorname{sech}(hD_x)$  implies that an assumption of regularity of the bottom  $\beta(x)$  is not needed, and our analysis is valid for any  $\beta \in C(\mathbb{R}_x)$ . A general setting of this form of transformation theory is given in Craig, Guyenne & Kalisch (2005), and the details of this particular calculation appear in de Bouard *et al.* (2008) and Craig & Sulem (to appear).

## 2.2. Change of variables and model equations

Our focus is on the KdV scaling regime. Changing coordinates, we define

$$\left. \begin{aligned} r &= \sqrt[4]{\frac{g}{4h_\varepsilon}} \eta - \sqrt[4]{\frac{h_\varepsilon}{4g}} u, \\ s &= -\sqrt[4]{\frac{g}{4h_\varepsilon}} \eta - \sqrt[4]{\frac{h_\varepsilon}{4g}} u, \end{aligned} \right\} \quad (2.19)$$

where  $(r, s)$  are solution components which propagate principally to the right and left respectively. Consider solutions which propagate principally to the right, which is to say that  $r$  is the dominant component, setting  $r = O(1)$  while the scattered component  $s = \varepsilon^{3/2}s_1$  is small. The scaling of the scattered component is a consequence of the Donsker invariance principle (an extension of the central limit theorem). In the scaling regime we discuss, the random bottom perturbations are  $O(\varepsilon)$  and are of zero mean value; hence the first-term correction to this is  $O(\varepsilon^{3/2})$ , with a coefficient proportional to the variance of the underlying process. The amplitude of the scattered component is directly related to this quantity. Rewrite (2.13) accordingly. In the resulting equations, we identify those terms which will play a role in the asymptotic limit as  $\varepsilon \rightarrow 0$ . This process leads to the following systems of model equations for the free surface in this scaling regime:

$$\partial_t r = -\partial_x \left[ c_\varepsilon(X)r + \varepsilon^2 \left( c_1 \partial_x^2 r + \frac{3}{2} c_2 r^2 \right) \right] + \varepsilon^2 b r + \varepsilon^2 R_\varepsilon, \quad (2.20)$$

$$\partial_t s_1 = \sqrt{gh} \partial_x s_1 + \frac{1}{4} \sqrt{\frac{g}{h}} \varepsilon^{-3/2} \partial_x \gamma \left( \frac{X}{\varepsilon} \right) r + S_\varepsilon, \quad (2.21)$$

where the regularized velocity is defined to be

$$c_\varepsilon(X) = \sqrt{gh} \left( 1 - \frac{\varepsilon}{2h} \gamma \left( \frac{X}{\varepsilon} \right) - \varepsilon^2 a \right) \quad (2.22)$$

and where the status of the remaining terms  $R_\varepsilon$  and  $S_\varepsilon$  is to be considered further. There are two free parameters in these equations, namely  $b$  and  $a$ . Set  $R_\varepsilon = 0 = S_\varepsilon$  in (2.20)–(2.21), and solve this system of equations. In order that the solution is consistent with the asymptotic reduction of Hamilton's equations,  $R_\varepsilon$  and  $S_\varepsilon$  must be shown to be of  $o(1)$  when calculated on a solution. This is accomplished when the two parameters are chosen with the following values:

$$a = \frac{1}{2h} a_\beta + \frac{1}{4h^2} \mathbf{E}(\gamma^2) + \frac{1}{8} \mathbf{E}((\partial_x \gamma)^2), \quad (2.23)$$

$$b = -\frac{1}{6 \times 16} \frac{7}{8} \sqrt{\frac{g}{h}} \mathbf{E}((\partial_x \gamma)^3). \quad (2.24)$$

We remark that  $a > 0$ , since  $a_\beta = \mathbf{E}(\beta D_x \tanh(h D_x) \beta) > 0$  for non-constant  $\beta$ , and therefore the average linear velocity of (2.13) is slowed with respect to the velocity of the solution in a channel of fixed depth  $h$ . With the above choice of parameters  $a$  and  $b$  solutions of (2.3) are modelled by the coupled system

$$\partial_t r = -\partial_x \left[ c_\varepsilon(X)r + \varepsilon^2 \left( c_1 \partial_x^2 r + \frac{3}{2} c_2 r^2 \right) \right] + \varepsilon^2 b r, \quad (2.25)$$

$$\partial_t s_1 = \sqrt{gh} \partial_x s_1 + \frac{1}{4} \sqrt{\frac{g}{h}} \varepsilon^{-3/2} \partial_x \gamma \left( \frac{X}{\varepsilon} \right) r. \quad (2.26)$$

We remark that (2.25) has a term involving  $b$  appearing at  $O(\varepsilon^2)$ , while (2.26) does not. Indeed a non-zero factor  $b$  would influence the scattered component  $s_1$  as well, also at  $O(\varepsilon^2)$ . This precision is however more than we have maintained for other contributions to the scattered component, and we have chosen to retain only the principal order of approximation, namely at  $O(\varepsilon^{3/2})$ . More details are given in de Bouard *et al.* (2008) and Craig & Sulem (to appear).

### 3. Random solutions and their limiting distributions

In this section we give a procedure for solving (2.25) and (2.26), and we analyse the behaviour of these solutions as  $\varepsilon$  tends to zero. The solutions depend upon the two parameters  $a$  and  $b$ ; if these are set to the values given in (2.23) and (2.24), then equations (2.25) and (2.26) represent the leading-order terms of (2.20) and (2.21). In other words, neglected terms are validated *a posteriori*; this is the structure of the self-consistency analysis of the problem. This procedure requires an analysis of the stationary processes of the problem and their limits, an understanding of random scale separation and the construction of random characteristic coordinates.

#### 3.1. Stationary processes

Realizations  $\beta(x; \omega)$  of the bottom topography are taken from an ensemble  $\Omega$ , with a probability measure  $(\mathcal{M}, \mathbf{P})$  describing their statistics. For each realization, we will solve (2.20) and (2.21). The random process is assumed to be stationary, meaning that  $\beta(x; \omega)$  and  $\beta(x + y; \omega) = (\tau_y \beta)(x; \omega)$  have the same statistical properties for any translation  $y$ . Without loss of generality, let

$$\mathbf{E}(\beta) := \int_{\Omega} \beta \, d\mathbf{P} = 0. \quad (3.1)$$

We assume that the process  $\beta(x; \omega)$  exhibits asymptotic independence under translation, which is the property of mixing. That is with respect to the probability measure  $\mathbf{P}$ , the local information given through observations  $A$  of  $\beta(x; \omega)$  over a window  $a_1 < x < a_2$  and information  $B$  over a window  $b_1 < x < b_2$ , translated by  $y$ , are statistically independent in the limit as  $y \rightarrow +\infty$ . Denoting the translation of the window  $B$  by  $\tau_y(B) = \{b_1 + y < x < b_2 + y\}$ , one quantifies the rate of decorrelation, or ‘mixing’, as follows:

$$|\mathbf{P}(A \cap \tau_y(B)) - \mathbf{P}(A)\mathbf{P}(B)| < \alpha(y). \quad (3.2)$$

For technical reasons, we ask that the decorrelation of events is sufficiently strong so that

$$\int_0^{\infty} \alpha^{1/2}(y) \, dy < +\infty. \quad (3.3)$$

Mixing implies ergodicity, among other things, and in particular for any bounded measurable function  $F : \Omega \rightarrow \mathbb{R}$ , for  $\mathbf{P}$ -almost every realization  $\beta$ ,

$$\lim_{L \rightarrow \infty} \frac{1}{L} \int_0^L F(\tau_y \beta) \, dy = \mathbf{E}(F). \quad (3.4)$$

The covariance function of the process is

$$\rho_{\beta}(y) := \mathbf{E}(\beta(0)\beta(y)), \quad (3.5)$$

and a second consequence of (3.3) on the mixing rate is that the variance

$$\sigma_{\beta}^2 := 2 \int_0^{\infty} \rho_{\beta}(y) \, dy \quad (3.6)$$

is finite. The hypotheses of stationarity and mixing make the problem very different from the periodic case studied in Rosales & Papanicolaou (1983) and Craig *et al.* (2005). We will assume in the present analysis that  $\sigma_{\beta} > 0$ , which also differs from Rosales & Papanicolaou (1983).

## 3.2. Averaging and scale separation

The most important effects of the randomness are given by products  $\mu(X/\varepsilon)f(X)$ , where  $\mu$  is a stationary mixing process and  $f$  is deterministic and a function of the large spatial scale. These occur in (2.20) and (2.21), for example.

**THEOREM 3.1.** *Suppose that  $f(X)$  is a Schwartz class test function. Then, for  $\varepsilon$  small,*

$$\int \mu\left(\frac{X}{\varepsilon}\right) f(X) dX = \int (\mathbf{E}(\mu) + \sqrt{\varepsilon}\sigma_\mu \partial_X B_\omega(X)) f(X) dX + o(\sqrt{\varepsilon}), \quad (3.7)$$

in the sense of convergence in law, where  $B_\omega(X)$  is normal Brownian motion.

This is the exhibition of the separation of scales; the first asymptotic term follows from the ergodic theorem, while the second is based on Donsker's invariance principle. The implication is that the asymptotic behaviour of the expression does not converge to a single value, but it is distributed normally, characterized by the two parameters  $\mathbf{E}(\mu)$  and  $\sigma_\mu^2$ . If  $\mu(x) = \partial_x \nu(x)$  in which  $\nu(x)$  is another such process, then  $\sigma_\mu = 0$ . The result is related to the work of Bal (2008), in which similar random corrections to homogenization theory are shown to be Gaussian through the generalized form of the central limit theorem. The proof of the above theorem appears in de Bouard *et al.* (2008), along with other limit theorems. For completeness, we give a sketch of the basic argument in the Appendix.

As an illustration of the theorem, let  $\mathbf{E}(\mu) = 0$  and consider the random variables

$$Z_\varepsilon(f) = \frac{1}{\sqrt{\varepsilon}} \int_{-\infty}^{+\infty} \mu\left(\frac{X}{\varepsilon}\right) f(X) dX. \quad (3.8)$$

In the limit as  $\varepsilon$  tends to zero, its covariance is

$$\mathbf{E}(Z_0(f)Z_0(g)) = \sigma_\mu^2 \int f(X)g(X) dX. \quad (3.9)$$

Indeed, we have

$$\begin{aligned} \mathbf{E}(Z_\varepsilon(f)Z_\varepsilon(g)) &= \frac{1}{\varepsilon} \int \int \rho_\mu\left(\frac{X-X'}{\varepsilon}\right) f(X)g(X') dXdX' \\ &= \int \int \rho_\mu(x') f(X)g(X-\varepsilon x') dXd x' \\ &= \int \int \rho_\mu(x') f(X) \left( g(X) - \varepsilon x' \partial_X g(X) + \frac{\varepsilon^2}{2} x'^2 \partial_X^2 g(X) + \dots \right) dX dx'. \end{aligned} \quad (3.10)$$

Noting that the term at  $O(\varepsilon)$  vanishes because  $\rho_\mu$  is an even function, we have

$$\mathbf{E}(Z_\varepsilon(f)Z_\varepsilon(g)) = \int \rho_\mu(x') dx' \int f(X)g(X) dX + O(\varepsilon^2), \quad (3.11)$$

which is consistent with the fact that the stationary process of 'white noise'  $\sigma_\mu \partial_X B_\omega(X)$  has covariance  $\sigma_\mu^2 \delta(X-X')$ .

## 3.3. Random characteristics and solutions

Using result (3.7) of the previous section, the asymptotic random wave speed (2.22) as  $\varepsilon \rightarrow 0$  is given by

$$c_0(X, \omega) = \sqrt{gh} \left( 1 - \frac{\varepsilon^{3/2} \sigma_\nu}{2h} \partial_X B_\omega(X) - \varepsilon^2 a \right), \quad (3.12)$$

where  $\gamma = \operatorname{sech}(hD_x)\beta$ , and we remark that a short calculation shows that  $\sigma_\gamma = \sigma_\beta$ . However, working with this expression directly is problematic, as the coefficients are too singular for techniques of stochastic differential equations. The natural regularization for the characteristic vector field for (2.20) is

$$\frac{dX}{dt} = c_\varepsilon(X, \omega), \quad X(0) = Y, \quad (3.13)$$

where  $c_\varepsilon = \sqrt{gh}(1 - (\varepsilon/2h)\gamma(X/\varepsilon) - \varepsilon^2 a)$  is given in (2.22). Since  $\operatorname{sech}(hD_x)$  is a smoothing operator,  $\gamma \in C^\infty$ . The characteristic flow of (3.13) is described by

$$X(t, Y; \varepsilon) = (Y + t\sqrt{gh}) - \frac{\varepsilon^2}{2h} \int_{Y/\varepsilon}^{(Y+t\sqrt{gh})/\varepsilon} \gamma(s, \omega) ds - \sqrt{gh} \left( a + \frac{1}{4h^2} \mathbf{E}(\gamma^2) \right) \varepsilon^2 t + \dots \quad (3.14)$$

As  $\varepsilon$  tends to zero, the characteristics tend to the limiting distribution

$$X(t, Y) = Y + t\sqrt{gh} - \frac{\varepsilon^{3/2}\sigma_\beta}{2h} \sqrt{gh} B_{\omega(Y)}(t) - \varepsilon^2 \sqrt{gh} \left( a + \frac{1}{4h^2} \mathbf{E}(\gamma^2) \right) t, \quad (3.15)$$

which describes straight-line trajectories perturbed by Brownian motion. For  $Y_1 \neq Y_2$ ,  $B_{\omega(Y_1)}$  and  $B_{\omega(Y_2)}$  are independent Brownian paths as long as  $t\sqrt{gh} < |Y_1 - Y_2|$ .

In characteristic coordinates, there is an explicit deterministic expression for (2.20). Define  $r = \partial_X R$  and  $Q(Y, \tau) = R(X, t)$  for  $\tau = \varepsilon^2 t$ . Then up to terms  $o(1)$  in  $\varepsilon$ ,  $Q$  satisfies the equation

$$\partial_\tau Q = -c_1 \partial_Y^3 Q - \frac{3}{2} c_2 (\partial_Y Q)^2 + bQ \quad (3.16)$$

in the sense of criterion (2.12). The quantity  $q(Y, \tau) = \partial_Y Q(Y, \tau)$  satisfies  $q(Y, 0) = r(Y, 0) = r^0(Y)$ ; the initial data for (2.20) and

$$\partial_\tau q = -c_1 \partial_Y^3 q - 3c_2 q \partial_Y q + bq \quad (3.17)$$

holds. Inverting this transformation, an expression of the resulting approximate solution  $r_\varepsilon(X, t)$  for fixed  $\varepsilon > 0$  is

$$r_\varepsilon(X, t) = \partial_X Q(Y(t, X; \varepsilon, \omega), \varepsilon^2 t) = \partial_Y Q(Y(t, X; \varepsilon, \omega), \varepsilon^2 t) \partial_X Y(t, X; \varepsilon, \omega). \quad (3.18)$$

Denoting  $R^{(0)}(X, t) = Q(X - \sqrt{gh}t, \varepsilon^2 t)$ ,

$$r_\varepsilon(X, t) = \partial_X \left( R^{(0)} \left( X + \frac{\varepsilon^2}{2h} \int_{(X-\sqrt{gh}t)/\varepsilon}^{X/\varepsilon} \gamma(\theta) d\theta, t \right) \right), \quad (3.19)$$

which is an expression in the form of the derivative of a deterministic function evaluated along a random curve. An expansion in powers of  $\varepsilon$  describes the asymptotic limit of this expression,

$$\begin{aligned} r(X, t) &= \partial_X \left( R^{(0)} \left( X + \frac{\varepsilon^{3/2}\sigma_\beta}{2h} \sqrt{gh} B_{\omega(X)}(t), t \right) \right) \\ &= R_X^{(0)} \left( X + \frac{\varepsilon^{3/2}\sigma_\beta}{2h} \sqrt{gh} B_{\omega(X)}(t), t \right) \left( 1 + \frac{\varepsilon^{3/2}\sigma_\beta}{2h} \sqrt{gh} \partial_X B_{\omega}(t) \right). \end{aligned} \quad (3.20)$$

The scattered component is

$$s_1(X, t) = s_1^0(X + \sqrt{gh}t) + \frac{\varepsilon^{-3/2}}{4h} \int_X^{X+\sqrt{gh}t} \partial_X \gamma \left( \frac{\theta}{\varepsilon} \right) r \left( \theta, t + \frac{X - \theta}{\sqrt{gh}} \right) d\theta, \quad (3.21)$$

with initial data  $s_1(X, 0) = s_1^0(X)$ . The random component of  $s_1$  appearing as the second term of (3.21) is expressed at lowest order by

$$\frac{\varepsilon^{-3/2}}{4h} \int_X^{X+\sqrt{ght}} \partial_x \gamma \left( \frac{\theta}{\varepsilon} \right) R_X^{(0)} \left( \theta, t + \frac{X-\theta}{\sqrt{gh}} \right) d\theta. \quad (3.22)$$

Using Theorem 3.1 and by integration by parts, we find that in the limit as  $\varepsilon \rightarrow 0$ , the asymptotic behaviour of the scattered component  $s_1$  is

$$\begin{aligned} s_1(X, t) = & s_1^0(X + \sqrt{ght}) - \frac{\sigma_\beta}{4h} \int_X^{X+\sqrt{ght}} \partial_\theta R_X^{(0)} \left( \theta, t + \frac{X-\theta}{\sqrt{gh}} \right) dB_\omega(\theta) \\ & - \frac{\sigma_\beta}{4h} (\partial_X B_\omega(X) R_X^{(0)}(X, t) - \partial_X B_\omega(X + \sqrt{ght}) R_X^{(0)}(X + \sqrt{ght}, 0)). \end{aligned} \quad (3.23)$$

The asymptotic behaviour of solution (3.20) is seen to be given by a deterministic function  $R_X^{(0)}$  whose phase is shifted in a random way by a Brownian motion at  $O(\varepsilon^{3/2})$ . In addition, the amplitude of the solution is modified by the Jacobian of the transformation to characteristic coordinates, which is in the form of a white noise, also at  $O(\varepsilon^{3/2})$ . The phase shift and the amplitude variations are correlated. The scattered component  $s_1(X, t)$  is given in (3.23) by a stochastic integral along a backward left-moving characteristic, with weight depending upon  $R^{(0)}$ , with additionally two impulsive sources due to interaction with the bottom, which are given in the limit by white noise. The statistics of the bottom appear in the solution only through the homogenized quantities  $a$  and  $b$  and the variance  $\sigma_\beta$ .

#### 3.4. Attenuation of solutions

A phenomenon which is exhibited by solutions of (3.17) is the occurrence of the additional linear term  $bq$ . This term results from multiple Bragg scattering of a solution with the rough bottom, and expression (2.24) for the coefficient  $b$  is an outcome of the consistency analysis of (2.20) and (2.21), in arriving at the model system (2.25) and (2.26). It represents  $O(1)$  contributions of the expressions  $R_\varepsilon$  and  $S_\varepsilon$  for the solution of the model equations, given the scale separation theorem. A full analysis of the Hamiltonian equations and their reduced form in the asymptotic limit is given in de Bouard *et al.* (2008).

If  $b=0$ , then (3.17) is the classical KdV equation. If the statistics of the ensemble  $(\Omega, \mathcal{M}, \mathbf{P})$  are reversible in  $x$ , meaning that the inversion  $\beta(x) \rightarrow \beta(-x)$  preserves the probability measure  $\mathbf{P}$ , then  $\gamma = \operatorname{sech}(hD_x)\beta$  satisfies  $\mathbf{E}((\partial_x \gamma)^3) = 0$ , implying  $b=0$ . However, for general stationary processes, this is not the case, and in particular a process with skew statistics results in a non-zero  $b$ . This is illustrated in figure 2, which is a configuration which attenuates wave propagation to the right.

The sign of  $b$  is significant to the long-time stability of solutions  $q(Y, \tau)$  of (3.17) and hence to the model equations. A straightforward indication of this is given by the behaviour of the  $L^2$ -norm of solutions:

$$\partial_\tau \int q^2 dY = 2b \int q^2 dY. \quad (3.24)$$

When  $b < 0$ , solutions are stable and the quantity  $\|q(\cdot, \tau)\|_2^2 = e^{2b\tau} \|q_0(\cdot)\|_2^2$  decays to zero. When  $b > 0$ , the same expression shows that the  $L^2$ -norm is growing with  $\tau$ , the usual time scale for the KdV equation.

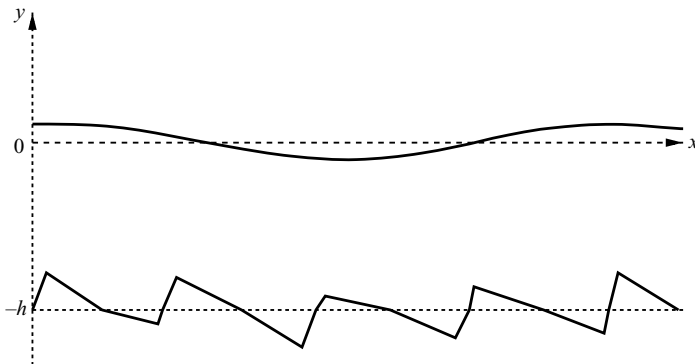


FIGURE 2. A sketch of a fluid domain with a bottom for which  $b = -(7/768)\sqrt{(g/h)}\mathbf{E}((\partial_x \beta)^3) < 0$ , which indicates that large positive slopes are more probable than large negative ones.

#### 4. Ensemble averages

We have focused on solutions  $r(X, t)$  of (2.20) for each realization  $\beta(\cdot; \omega)$  of the bottom. In the field of stochastic differential equations, it is common to study the expected value  $p(X, t) = \mathbf{E}(r(X, t))$  of these solutions, or their variance, or other quantities such as their higher moments, as standard statistical predictors of their behaviour.

As we discussed in §1, in the present problem there is a qualitative difference between solutions for an individual realization and the mean value; in particular the latter has the possibility of exhibiting diffusion (Nachbin & Sølna 2003) which the former does not. In this section, we show that diffusion is however a higher-order effect in the present scaling regime. Indeed taking the expected value of the regularized equation (2.20), we find

$$\partial_t p = -\partial_X \left[ \mathbf{E}(c_\varepsilon(X)r) + \varepsilon^2 \left( c_1 \partial_X^2 p + \frac{3}{2} c_2 \mathbf{E}(r^2) \right) \right] + \varepsilon^2 b p. \quad (4.1)$$

To leading order in  $\varepsilon$ ,  $\mathbf{E}(r^2) = p^2$  because of the character of (3.14). Computing  $\mathbf{E}(c_\varepsilon(X)r)$ , we use the expression

$$c_\varepsilon(X)r = \sqrt{gh} \left[ 1 - \frac{\varepsilon}{2h} \gamma \left( \frac{X}{\varepsilon} \right) - \varepsilon^2 a \right] \left[ q + \partial_X \left( q \frac{\varepsilon}{2h} \int_{X-\sqrt{gh}t}^X \gamma \left( \frac{\theta}{\varepsilon} \right) d\theta \right) \right]. \quad (4.2)$$

The main contribution is therefore  $\sqrt{gh} \partial_X p$ . Using that  $\gamma$  is of zero mean, the principal non-trivial higher-order contribution to  $\mathbf{E}(c_\varepsilon(X)r)$  comes from the term

$$-\sqrt{gh} \frac{\varepsilon}{2h} \gamma \partial_X \left( q \frac{\varepsilon^2}{2h} \int_{(X-\sqrt{gh}t)/\varepsilon}^{X/\varepsilon} \gamma(\theta) d\theta \right). \quad (4.3)$$

Thus

$$\begin{aligned} \mathbf{E}(c_\varepsilon(X)r) &= \sqrt{gh} (1 - \varepsilon^2 a) p - \sqrt{gh} \frac{\varepsilon^2}{4h^2} \left( \mathbf{E}(\gamma^2) - \rho_\gamma \left( \frac{t\sqrt{gh}}{\varepsilon} \right) \right) p \\ &\quad - \sqrt{gh} \frac{\varepsilon^3}{4h^2} \partial_X p \int_{(X-\sqrt{gh}t)/\varepsilon}^{X/\varepsilon} \rho_\gamma \left( \theta - \frac{X}{\varepsilon} \right) d\theta + o(\varepsilon^2), \end{aligned} \quad (4.4)$$

where  $\rho_\gamma$  is the covariance of the process  $\gamma$ . As  $\varepsilon \rightarrow 0$ , the mixing rate implies that  $\rho_\gamma(t\sqrt{gh}/\varepsilon) \rightarrow 0$ . Thus,

$$\begin{aligned} \mathbf{E}(c_\varepsilon(X)r) &= \sqrt{gh} \left( 1 - \varepsilon^2 \left( a + \frac{1}{4h^2} \mathbf{E}(\gamma^2) \right) \right) p \\ &\quad - \sqrt{gh} \frac{\varepsilon^3}{4h^2} \partial_X p \int_{-\sqrt{gh}t/\varepsilon}^0 \rho_\gamma(\theta) d\theta. \end{aligned} \quad (4.5)$$

In the limit as  $\varepsilon \rightarrow 0$ , the asymptotic behaviour of this expression is

$$\sqrt{gh}p - \varepsilon^2 \sqrt{gh} \left( a + \frac{1}{4h^2} \mathbf{E}(\gamma^2) \right) p - \sqrt{gh} \frac{\varepsilon^3}{8h^2} \sigma_\beta^2 \partial_X p. \quad (4.6)$$

Therefore asymptotically, the expected value  $p(X, t)$  obeys an equation of the form

$$\begin{aligned} \partial_t p &= -\sqrt{gh} \left[ 1 - \varepsilon^2 \left( a + \frac{1}{4h^2} \mathbf{E}(\gamma^2) \right) \right] \partial_X p - \varepsilon^2 (c_1 \partial_X^3 p + 3c_2 p \partial_X p) \\ &\quad + \sqrt{gh} \frac{\varepsilon^3}{8h^2} \sigma_\beta^2 \partial_X^2 p + \varepsilon^2 b p + o(\varepsilon^2), \end{aligned} \quad (4.7)$$

in which the diffusion appears at  $O(\varepsilon^3)$ . It therefore does not play a significant role in this scaling regime at the order of the calculations of §3.

In Nachbin & Sølna (2003), the authors have studied (2.1) and (2.3), linearized and in the shallow-water regime, with rapidly varying topography. In contrast to the present work in which the bottom is in the form  $y = -h + \varepsilon\beta(X/\varepsilon)$ , they have admitted larger bottom variations, of amplitude  $\sqrt{\varepsilon}$ . In their linear analysis, the expected value of their solutions is shown to exhibit diffusive behaviour at  $O(\varepsilon^2)$ . In the nonlinear problem, this scaling of the bottom variations will introduce many additional terms into the asymptotic analysis, whose effects must be understood. It would be an interesting future study to extend the nonlinear analysis to this situation.

## 5. Slowly varying statistics

We now extend our analysis to the more general case in which the bottom varies both on a length scale of  $O(1)$  and on a longer scale. An illustration is given in figure 3. As in previous sections, the topography of the bottom is described by its variations from constant depth  $\beta = \beta(x, X, \varepsilon; \omega)$ , which is taken from a statistical ensemble of realizations. One may always decompose  $\beta = \beta_0 + \beta_1$ , where  $\beta_0(X, \varepsilon)$  is deterministic and  $\beta_1 = \beta_1(x, X, \varepsilon; \omega)$  represents random variations in the short spatial scale with zero mean value.

Introducing a local corrected depth,

$$h_\varepsilon(X) = h - \varepsilon\beta_0(X) - \varepsilon\gamma_1(X/\varepsilon, X) - \varepsilon^2 a_{\beta_1}(X),$$

where  $\gamma_1(x, X) = \text{sech}(hD_x)\beta_1$  and  $a_{\beta_1}(X) = \mathbf{E}(\beta_1(\cdot, X, \varepsilon)(D_x \tanh(hD_x)\beta_1)(\cdot, X, \varepsilon))$  and where we have used the fact that  $\text{sech}(hD_x)\beta_0(X) = \beta_0(X) + O(\varepsilon^2)$ . As in §2.2, the resulting Hamiltonian is

$$H(\eta, u, \beta; \varepsilon) = \frac{\varepsilon^3}{2} \int (h_\varepsilon(X)u^2 + g\eta^2) dX + \frac{\varepsilon^5}{2} \int \left( \eta u^2 - \frac{h^3}{3} (\partial_X u)^2 \right) dX + o(\varepsilon^5). \quad (5.1)$$

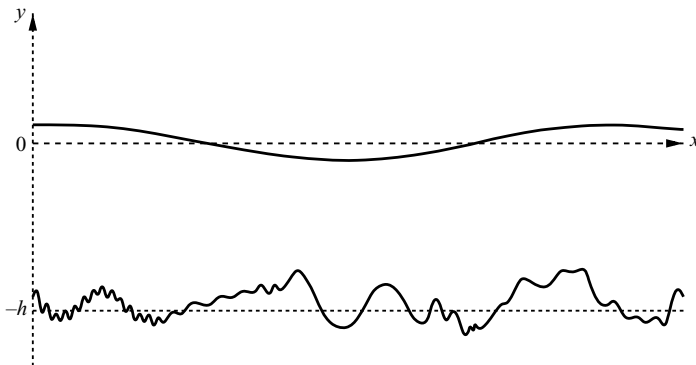


FIGURE 3. A sketch of long waves over a fluid domain with a random bottom with slowly varying statistical properties.

Transforming to scattering variables (2.19) and rescaling to anticipate a scattering situation in which right-moving solutions dominate, the analogous Hamiltonian is

$$H_2^\varepsilon = \frac{\varepsilon^3}{2} \int \left( \sqrt{gh_\varepsilon} (r^2 + \varepsilon^3 s_1^2) - \frac{\varepsilon^2 h^3}{3} (\partial_X (k_\varepsilon r - \varepsilon^{3/2} k_\varepsilon s_1))^2 + \frac{\varepsilon^2}{2} k_\varepsilon (r^3 - \varepsilon^{3/2} r^2 s_1 - \varepsilon^3 r s_1^2 + \varepsilon^{9/2} s_1^3) \right) dX + o(\varepsilon^5), \quad (5.2)$$

where  $k_\varepsilon(X) = \sqrt[4]{\frac{g}{4h_\varepsilon(X)}}$ .

### 5.1. Modulated averaging and scale separation

The situation in which the statistical component  $\beta_1 = 0$  is analysed in e.g. van Groesen & Pudjaprasetya (1993), and is one of the problems addressed in Craig *et al.* (2005). Our goal in this section is to discuss the case in which the topography of the bottom has short spatial scale variations, which have slowly varying statistical properties as well as a slowly varying mean value. Realizations of the bottom topography are given by functions  $\beta = \beta(x, X, \varepsilon; \omega)$  which represent families of stationary processes in  $x \in \mathbb{R}_x$  parameterized by the long-scale variables  $X \in \mathbb{R}_X$ . We take  $\beta \in C(\mathbb{R}_X; \Omega)$ , where  $\Omega = C(\mathbb{R}_x)$  such that  $\beta(\cdot, X, \varepsilon; \omega)$  is a stationary ergodic process in  $x \in \mathbb{R}_x$  with translation-invariant probability measure  $\mathbf{P}(X)$ . We assume that  $\mathbf{P}(X)$  is weakly continuous in  $X$  and that the family of processes is jointly mixing with a uniform and sufficiently fast rate. Then the model for multiple-scale bathymetry is to set the bottom variations to  $\beta = \beta(X/\varepsilon, X, \varepsilon; \omega)$ . Details of this construction and results on its statistical behaviour are given in the Appendix.

The mean value of  $\beta$  is given by

$$\beta_0(X, \varepsilon) = \int_{\Omega} \beta(\cdot, X, \varepsilon; \omega) d\mathbf{P}(X) := \mathbf{E}_X(\beta(\cdot, X)),$$

so that  $\beta_1 = \beta - \beta_0$  is of zero mean value. The variance  $\sigma_{\beta_1}(X)$  of this process is defined by a limiting argument that is sketched in the Appendix. The effect is that the asymptotics of the integrals such as given in (3.7) is modified, described by an analogue to Theorem 3.1.

**THEOREM 5.1.** *Consider  $\mu(x, X)$  a family of jointly stationary mixing processes as introduced above, and assume that the variance  $\sigma_\mu(X)$  is bounded and bounded away*

from zero. Let  $f(X)$  be a Schwartz class test function. Then for small  $\varepsilon$ ,

$$\int f(X) \mu \left( \frac{X}{\varepsilon}, X \right) dX = \int f(X) \mathbf{E}(\mu)(X) dX + \sqrt{\varepsilon} \int f(X) \sigma_\mu(X) dB_\omega(X) + o(\sqrt{\varepsilon}), \quad (5.3)$$

in the sense of convergence in law.

This result follows from Donsker's invariance principle with an argument related to that of Theorem 3.1; the proof is given in the Appendix.

### 5.2. Derivation of the asymptotic equations

Following the steps of §3, we derive a system of reduced equations for  $r$  and  $s_1$  of the form

$$\partial_t r = -\partial_X \left( c_\varepsilon(X) r + \varepsilon^2 \left( c_1 \partial_X^2 r + \frac{3}{2} c_2 r^2 \right) \right) + \varepsilon^2 b(X) r + \varepsilon^2 R_\varepsilon, \quad (5.4)$$

$$\partial_t s_1 = \partial_X (c_\varepsilon(X) s_1) + \frac{1}{4} \sqrt{\frac{g}{h}} \varepsilon^{-3/2} \left( \varepsilon \partial_X \beta_0 + (\partial_X + \varepsilon \partial_X) \gamma_1 \left( \frac{X}{\varepsilon}, X \right) \right) r + S_\varepsilon, \quad (5.5)$$

where  $R_\varepsilon$  and  $S_\varepsilon$  are  $o(1)$ . In (5.4) and (5.5), the regularized wave speed  $c_\varepsilon$  is given by

$$c_\varepsilon(X) = \sqrt{gh} \left( 1 - \frac{\varepsilon}{2h} (\beta_0 + \gamma_1) - \varepsilon^2 a(X) \right). \quad (5.6)$$

We assume that the variations of the deterministic component of the bottom varies on scales longer than those of the surface elevation  $\partial_X \beta_0(X) = o(\varepsilon^{1/2})$  (van Groesen & Pudjaprasetya 1993). A physical situation in which this occurs is for example for long waves propagating over a slowly varying beach slope. The implication of this hypothesis is that the presence of a slowly varying mean value  $\beta_0(X)$  of  $\beta(x, X)$  does not significantly change the conclusions of the analysis.

The parameters  $a(X)$  and  $b(X)$  are slowly varying functions that are determined through a consistency analysis, yielding

$$a(X) = \frac{1}{2h} a_{\beta_1} + \frac{1}{8h^2} (\beta_0^2 + 2\mathbf{E}(\gamma_1^2)) + \frac{1}{8} \mathbf{E}((\partial_X \gamma_1)^2), \quad (5.7)$$

$$b(X) = -\frac{1}{16h} \sqrt{\frac{g}{h}} \partial_X \mathbf{E}(\gamma_1^2) - \frac{1}{16} \sqrt{gh} \partial_X \mathbf{E}((\partial_X \gamma_1)^2) - \frac{1}{6 \times 16 \times 8} \sqrt{\frac{g}{h}} \mathbf{E}((\partial_X \gamma_1)^3), \quad (5.8)$$

where  $a_{\beta_1}(X) = \mathbf{E}(\beta_1 D_x \tanh(h D_x) \beta_1)$ .

If  $\beta_0 = 0$  and the statistics of  $\beta_1$  are fixed, then (5.7) and (5.8) reduce to (2.23) and (2.24) of the previous case. As before, the component  $r(X, t)$  is expressed in terms of a solution to a deterministic KdV-type equation through a random change of coordinates:

$$\begin{aligned} r_\varepsilon(X, t) &= \partial_Y Q \partial_X Y \\ &= q(X - \sqrt{ght}, \varepsilon^2 t) \\ &\quad + \partial_X \left( q(X - \sqrt{ght}, \varepsilon^2 t) \left( \frac{\varepsilon}{2h} \int_{X - \sqrt{ght}}^X \left( \beta_0(s) + \gamma_1 \left( \frac{s}{\varepsilon}, s \right) \right) ds \right) \right), \end{aligned} \quad (5.9)$$

where  $q$  satisfies

$$\partial_\tau q = -c_1 \partial_Y^3 q - 3c_2 q \partial_Y q + b \left( Y + \sqrt{gh} \frac{\tau}{\varepsilon^2} \right) q, \quad (5.10)$$

with  $\tau = \varepsilon^2 t$  and

$$\frac{dX}{dt} = c_\varepsilon(X, \omega), \quad X(0) = Y. \quad (5.11)$$

In (5.10), we note that the coefficient  $b$  depends on  $\varepsilon$  when expressed in terms of  $Y$  and  $\tau$ . We impose the additional hypothesis that the statistics of the bottom stabilize for large positive  $X$ , which implies that  $b(X)$  tends to a constant value  $b_0$ . We thus obtain a KdV equation with an additional linear term, of the form

$$\partial_\tau q = -c_1 \partial_Y^3 q - 3c_2 q \partial_Y q + b_0 q, \quad (5.12)$$

as in our prior analysis.

### 5.3. Random characteristics and limiting solutions

We solve (5.11) perturbatively. Write

$$X(t, Y) = Y + \sqrt{gh}t + \varepsilon Z, \quad (5.13)$$

where  $Z = Z_0 + \sqrt{\varepsilon} Z_1$ ; then at lowest order,

$$Z_0 = -\frac{1}{2h} \int_Y^{Y+\sqrt{gh}t} \beta_0(\theta) d\theta. \quad (5.14)$$

Furthermore, at next order, we have

$$\begin{aligned} \frac{dZ_1}{dt} = & -\frac{1}{2\sqrt{\varepsilon}} \sqrt{\frac{g}{h}} \gamma_1 \left( \frac{Y + \sqrt{gh}t}{\varepsilon} + Z_0, Y + \sqrt{gh}t \right) \\ & - \frac{1}{2} \sqrt{\frac{g}{h}} \partial_x \gamma_1 \left( \frac{Y + \sqrt{gh}t}{\varepsilon} + Z_0, Y + \sqrt{gh}t \right) Z_1, \end{aligned} \quad (5.15)$$

whose solution is given by

$$Z_1 = -\frac{1}{2h\sqrt{\varepsilon}} \int_Y^{Y+\sqrt{gh}t} \gamma_1 \left( \frac{\theta}{\varepsilon} + Z_0 \left( \frac{\theta - Y}{\sqrt{gh}} \right), \theta \right) d\theta + O(\varepsilon). \quad (5.16)$$

The limiting distribution of  $Z_1$  as  $\varepsilon$  tends to 0 is obtained as an application of Theorem 5.1. We find that

$$Z_1 = -\frac{1}{2h} \int_Y^{Y+\sqrt{gh}t} \sigma_{\beta_1}(\theta) dB_\omega(\theta) + o(1), \quad (5.17)$$

where  $B_\omega$  is a normal Brownian motion. The characteristic coordinates take the form, in the limit  $\varepsilon \rightarrow 0$ ,

$$X(t, Y) = Y + \sqrt{gh}t - \frac{\varepsilon}{2h} \int_Y^{Y+\sqrt{gh}t} \beta_0(\theta) d\theta - \frac{\varepsilon^{3/2}}{2h} \int_Y^{Y+\sqrt{gh}t} \sigma_{\beta_1}(\theta) dB_\omega(\theta) + o(\varepsilon^{3/2}) \quad (5.18)$$

or, equivalently,

$$Y(t, X) = X - \sqrt{gh}t + \frac{\varepsilon}{2h} \int_{X-\sqrt{gh}t}^X \beta_0(\theta) d\theta + \frac{\varepsilon^{3/2}}{2h} \int_{X-\sqrt{gh}t}^X \sigma_{\beta_1}(\theta) dB_\omega(\theta) + o(\varepsilon^{3/2}). \quad (5.19)$$

The Jacobian of the transformation to characteristic coordinates is expressed asymptotically as

$$\begin{aligned} \frac{dY}{dX} &\sim 1 + \frac{\varepsilon}{2h}(\beta_0(X) - \beta_0(X - \sqrt{ght})) \\ &\quad + \frac{\varepsilon^{3/2}}{2h}(\sigma_{\beta_1}(X)\partial_X B_\omega(X) - \sigma_{\beta_1}(X - \sqrt{ght})\partial_X B_\omega(X - \sqrt{ght})). \end{aligned} \quad (5.20)$$

Substitution of the above expression for random characteristic coordinates in (5.9) gives the form of the asymptotic solutions of (5.4),

$$r(X, t) = q(Y(t, X), \varepsilon^2 t) \frac{dY}{dX}. \quad (5.21)$$

This form of the solution exhibits phase translations given by a diffusion process about the classical trajectories and the modulation of the amplitude by two terms: a deterministic one and a random one which takes the form of a modulated white noise. The scattering term  $s_1$  is obtained by integration along left-moving characteristics which, to principal order, are given by straight-line motion at velocity  $-\sqrt{gh}$ , with a forcing term given by the interaction of the principal component  $r(X, t)$  and the bottom topography. The asymptotic behaviour of  $s_1$  is

$$\begin{aligned} s_1(X, t) &= s_1^0(X + \sqrt{ght}) - \frac{1}{4h} \int_X^{X+\sqrt{ght}} \sigma_{\beta_1}(\theta) \partial_\theta R_X^{(0)} \left( \theta, t + \frac{X - \theta}{\sqrt{gh}} \right) dB_\omega(\theta) \\ &\quad - \frac{1}{4h} (\sigma_{\beta_1}(X) \partial_X B_\omega(X) R_X^{(0)}(X, t) - \sigma_{\beta_1}(X + \sqrt{ght}) \partial_X \\ &\quad \times B_\omega(X + \sqrt{ght}) R_X^{(0)}(X + \sqrt{ght}, 0)), \end{aligned} \quad (5.22)$$

which is the analogue to (3.23) using Theorem 5.1.

## 6. Illustration of random effects with numerical simulations

In this section, we integrate numerically the model equations (2.25) and (2.26) for small but finite values of  $\varepsilon$ . System (2.25) and (2.26) consists of an equation similar to the KdV equation, coupled with a linear equation for the scattered component. Using the solution method of §3.3, expression (2.25) reduces to integrating a deterministic nonlinear equation in random characteristic coordinates. The scattering component is given by the integration of a transport equation along characteristics with a random forcing term.

### 6.1. Numerical model

The numerical simulations consist of three parts. The first part is deterministic: solve (3.17) for  $q(Y, \tau)$ . The second part introduces the random effects: perform the phase shift (3.14), and apply the Jacobian  $\partial_X Y$  which modulates the solution's amplitude, in order to obtain  $r(X, t)$ . The third part evaluates the scattered component  $s(X, t)$  and determines the free-surface elevation  $\eta(X, t)$  from  $r$  and  $s$ .

To solve (3.17), we consider a periodic domain of length  $L$  in the  $Y$ -direction and use a pseudo-spectral method for space discretization. More specifically,  $q$  is approximated by a truncated Fourier series with  $N$  modes. Differentiation in  $Y$  is performed in the Fourier space, while the nonlinear term is evaluated in physical space at a discrete set of  $N$  equally spaced points. These operations can be efficiently performed using the fast Fourier transform. Zero-padding is applied to suppress aliasing errors.

The integration in  $\tau$  is carried out in Fourier space, which allows the linear terms (i.e. the third-order dispersive term and the  $b$ -term) to be solved exactly by the integrating factor technique. For the integration of the nonlinear term, a fourth-order Runge–Kutta scheme with constant time step  $\Delta\tau$  is used. The corresponding values of  $t$  are obtained by the change of variables  $\tau = \varepsilon^2 t$ . Tests were conducted to assess the convergence of this numerical model, e.g. by checking the conservation of mass, energy and wave profile for a KdV soliton when  $b=0$ .

The phase shift (3.14) and the amplitude modulation  $\partial_x Y$  are computations involving  $\beta$ . Since  $\beta$  is a function of  $x$ , it is specified on an auxiliary domain of length  $l$  such that  $L = \varepsilon l$ . We have chosen a random model for the bathymetry such that a typical realization of the bottom has a sawtooth geometry (as shown in figure 2) in which a unit (a sawtooth) represents the characteristic (short) length scale of  $\beta$ . The amplitude of each unit is then assigned a random number which is uniformly distributed between  $-\varepsilon$  and  $\varepsilon$ . The back-and-forth asymmetry of the sawtooth geometry determines the sign of  $b$ .

In (3.14), the functions  $\gamma$ ,  $\partial_x \gamma$  and  $\beta D_x \tanh(h D_x) \beta$  are computed by pseudo-spectral method on the auxiliary  $x$ -domain, and their expected values are evaluated as spatially averaged values on this same domain. As for the integral term in  $\beta$ , it is approximated using the trapezoidal rule on the interval  $[Y/\varepsilon, (Y + t\sqrt{gh})/\varepsilon]$  (or equivalently  $[(X - t\sqrt{gh})/\varepsilon, X/\varepsilon]$ ) in which the endpoints are mapped to points in the auxiliary domain by nearest neighbour interpolation. For each  $Y$ , the transformation yields a value  $X$  (with the corresponding  $q$ ) which is then recast into the computational domain of length  $L$  using again nearest neighbour interpolation. We also used cubic spline interpolation and obtained similar results, which is probably due to the fact that a sufficiently fine spatial resolution was specified in our simulations. The Jacobian  $\partial_x Y$  is approximated by

$$\frac{\partial Y}{\partial X} = 1 + \frac{\varepsilon}{2h} \left[ \gamma \left( \frac{X}{\varepsilon} \right) - \gamma \left( \frac{X - t\sqrt{gh}}{\varepsilon} \right) \right]$$

and is evaluated by the same interpolation method.

The scattered component  $s$  is computed by integrating (2.26) for  $s_1$  using the trapezoidal rule, which is equivalent to evaluating the integral expression (3.21), and multiplying  $s_1$  by  $\varepsilon^{3/2}$ . The free-surface elevation  $\eta$  is then determined from  $r$  and  $s$  by inverting (2.19). All variables are non-dimensionalized according to long-wave theory; i.e. lengths are divided by a constant reference depth  $h_0$ , and times are divided by  $\sqrt{h_0/g}$  so that  $g = 1$ .

## 6.2. Numerical results

We performed simulations for  $\varepsilon = 0.1, 0.2$  and several realizations of the bottom topography. Smaller values of  $\varepsilon$  produce random effects of smaller amplitude and require the use of finer resolutions (thus a larger computational cost) in order to resolve the corresponding small-scale variations. Therefore, the small but finite values  $\varepsilon = 0.1, 0.2$  were found to be a good compromise for our numerical simulations.

We specified as initial condition a KdV soliton for the component  $r^0(X)$ , while  $s_1^0(X) = 0$ . A typical situation, with a realization of the bottom topography, is depicted in figure 4 for  $h = 1$  and  $\varepsilon = 0.2$ . The length scale of the bottom variations is chosen so that the width of the surface soliton corresponds to about  $1/\varepsilon = 5$  units of the bottom topography. For these parameter values, the coefficient  $b$  is very small in magnitude ( $b = -7.03 \times 10^{-5}$ ) and can be considered to be essentially indistinguishable from the case  $b = 0$ .

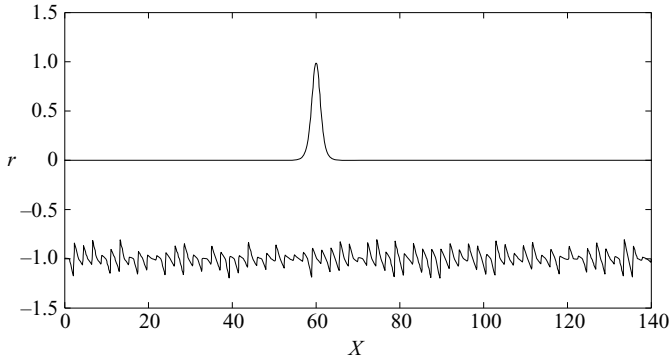


FIGURE 4. The upper curve represents the initial profile of  $r$ . The lower curve represents one realization of the bottom topography  $-h + \varepsilon\beta(x)$ . In this simulation,  $h = 1$  and  $\varepsilon = 0.2$ . The bottom topography is traced in actual scale relative to  $h$ , while the vertical scale for the initial profile has been magnified by a factor  $\varepsilon^{-2}$ .

Corresponding snapshots of the free surface at times  $t = 0, 12, 36, 60$  are shown in figure 5. The numerical parameters are  $L = 140$ ,  $N = 8192$  and  $\Delta\tau = 10^{-3}$ . The basic effect which is exhibited is that a coherent nonlinear wave propagates without significant deformation and attenuation over the interval of time considered. The development of scattering is evident and is clearly distinguished from the principal component in the decomposition given in figure 6. We see that the scattered component is of much smaller amplitude than the principal one and propagates in the opposite direction as expected.

In order to illustrate more clearly the effects of the random bottom on the principal component, figure 7 presents a close-up of the profiles of figure 6 near the soliton. It shows small displacements of the crest due to phase modulation, as well as profile deformations.

The phase modulation is revealed more clearly in figure 8 which shows space-time curves describing the deviation in position of the crest of  $r$  with respect to a soliton unperturbed by bottom variations. The three curves represent three different realizations of the bottom geometry, and their irregular oscillations are consistent with Brownian motion. Figure 9 represents the deviation of the centre of mass for the same three realizations. These curves are smoother than their counterparts in figure 8, but overall, they follow similar random trajectories. Here, we used a finer resolution ( $N = 16384$ ) to capture these deviations more accurately.

In the previous simulations, the coefficient  $b$  is so small in magnitude that its effect is not noticeable, even over long intervals of time. Considering a set of simulations with markedly skewed statistics of the triangular basic bottom geometry, and with a smaller ratio (average depth/characteristic bottom length scale), we obtain more significant values of the parameter  $b$ . This situation is illustrated in figure 10 which shows a realization of the bottom topography (with  $b < 0$ ) together with snapshots of the free surface for  $h = 1/4$  and  $\varepsilon = 0.1$ . The numerical parameters are  $L = 20$ ,  $N = 1024$  and  $\Delta\tau = 2 \times 10^{-4}$ . Note here that the height and width of the soliton are smaller than in the previous situation because  $h$  is smaller, and the length scale of the bottom variations relative to the soliton width is also shorter than previously because  $\varepsilon$  is smaller. For these parameter values,  $b = -8.85 \times 10^{-3}$ , and we note that it is negative. As expected, it can be seen that the solution's amplitude decreases, an effect which we have illustrated over a long interval of time ( $O(10^3)$ ). This amplitude

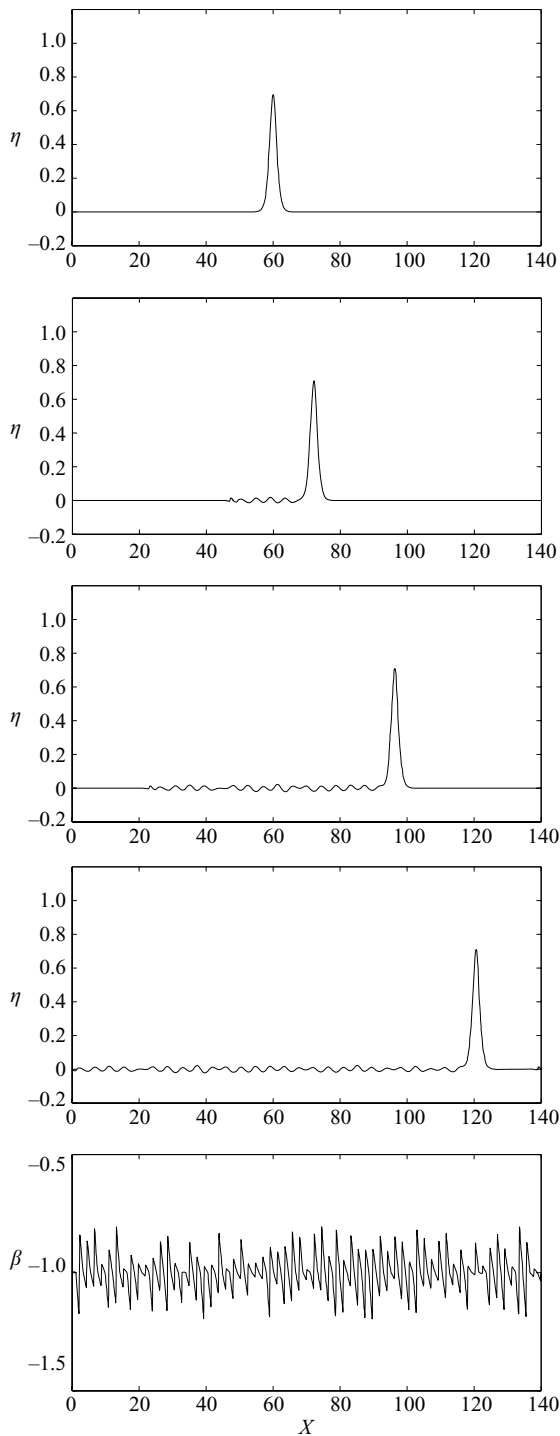


FIGURE 5. Profiles of the free surface  $\eta$  for  $\varepsilon=0.2$  ( $h=1$ ) at  $t=0, 12, 36, 60$  showing the development of a scattered component. The vertical scale has been enlarged by a factor  $\varepsilon^{-2}$ . The lower panel represents the corresponding bottom geometry.

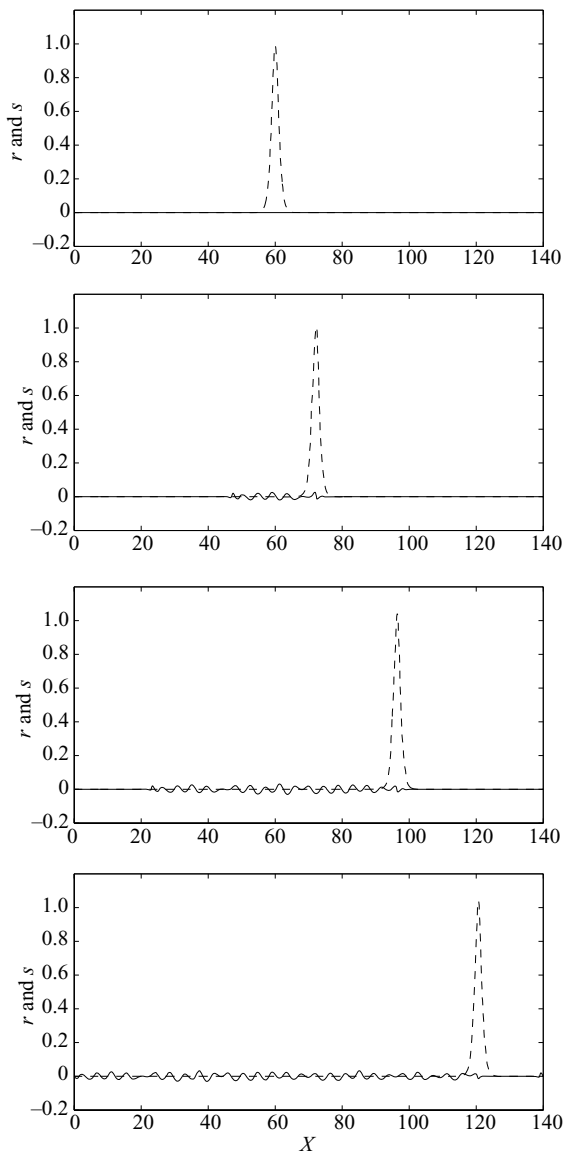


FIGURE 6. Decomposition into principal and scattered components of the simulation described in figure 5. Profiles of  $r$  (dashed line) and  $s$  (solid line) are given at the sequence of times  $t = 0, 12, 36, 60$ .

decrease is indicated more clearly in figure 11 which shows the time evolution of the profile of  $r$  and in figure 12 which presents the time evolution of the  $L^2$ -norm of  $r$ . The exponential decay of the solution is especially apparent in the latter figure.

## 7. Conclusions

This paper studies surface water waves in a fluid domain with a randomly varying bottom. We describe the asymptotic regime of small-amplitude long waves, for which

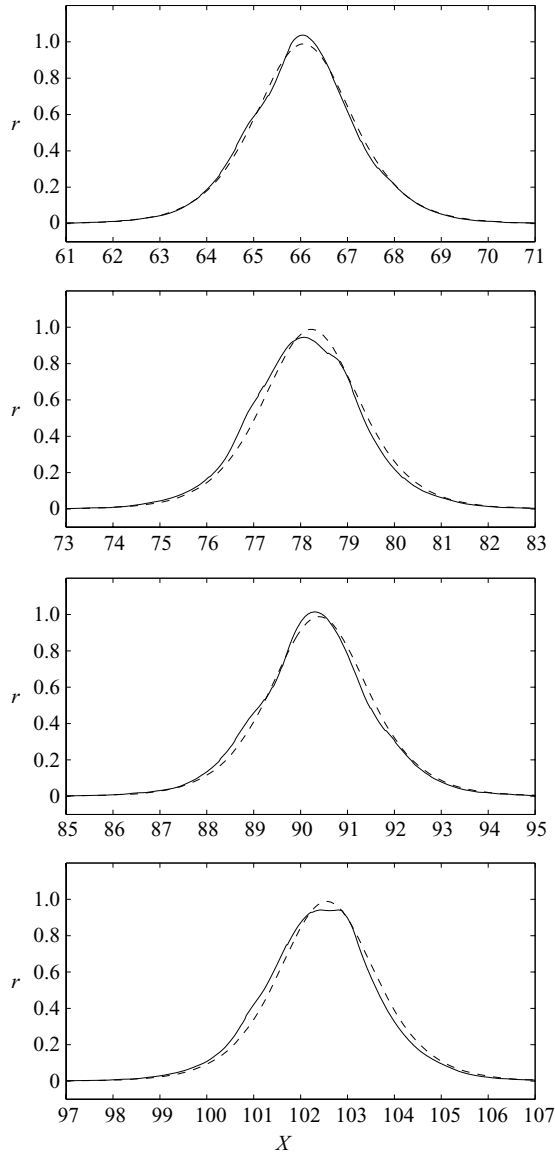


FIGURE 7. Details of the evolution near the peak of the principal component  $r$  (solid line) compared with the reference solution computed with flat bottom (dashed line) at  $t = 6, 18, 30, 42$ .

the correlation length of the bottom is short compared to the wavelength. We first consider the case in which the bottom is random with uniform statistical properties. In this regime, random effects are equally or more important than nonlinear and dispersive ones. We then extend our analysis to the case in which the bottom has large-scale deterministic variations as well as small-scale random fluctuations, whose statistical properties are allowed to vary slowly.

We find that the problem does not fully homogenize and that one sees important contributions to the solution which are realization dependent. Nevertheless, in the KdV limiting regime, there is an essentially explicit solution method which exhibits

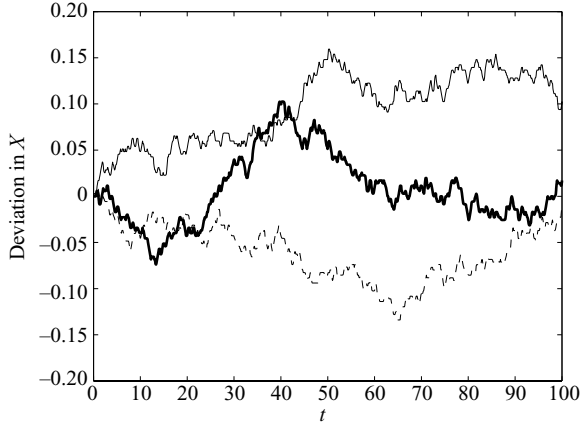


FIGURE 8. Variation of the position of the crest of the principal component  $r$ , relative to that of the reference solution with flat bottom, for three different realizations of the bottom topography ( $h = 1$ ,  $\varepsilon = 0.2$ ).

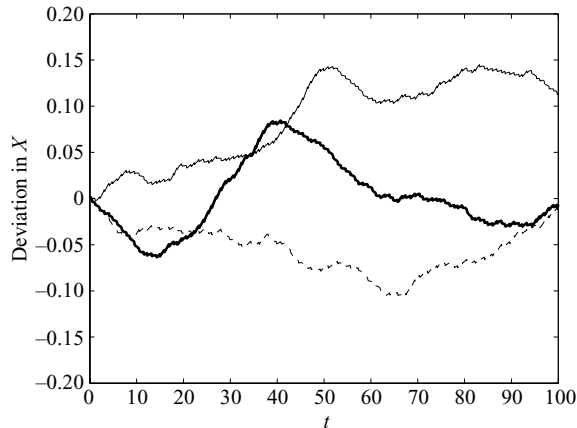


FIGURE 9. Variation of the centre of mass of the principal component  $r$  in the same situation as in figure 8, exhibiting smoother behaviour.

the principal features of the problem. We show that coherent wave-like solutions persist, and they maintain in many cases the same basic properties of momentum and energy transport as in the classical problem of a flat bottom. However these solutions are modified by two random and realization-dependent effects. First, the phase of the solutions has a random component which, in the asymptotic limit, is governed by a canonical diffusion process, essentially a Brownian motion. This is as in the work of Rosales & Papanicolaou (1983) and Garnier *et al.* (2007). Second, there is a modulation of the solutions' amplitude by a white noise process. These two manifestations of randomness are correlated. This quantifies the degree of uncertainty in determining the phase and amplitude of nonlinear waves over a random bottom. Wave propagation over a variable bottom gives rise to scattered wave fields. We quantify the scattered solution in our scaling regime; we express it in explicit form in terms of a related diffusion process which is a weighted integral of white noise; and

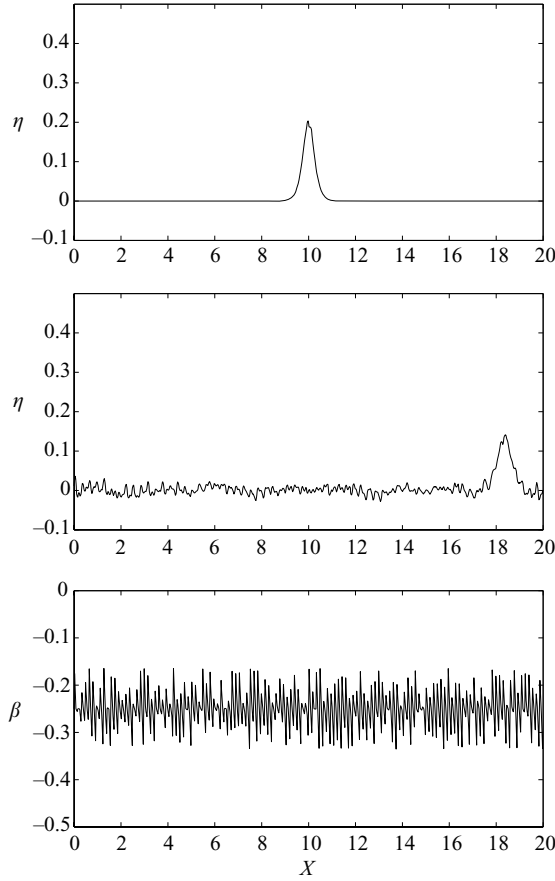


FIGURE 10. Profiles of the free surface  $\eta$  for  $\varepsilon=0.1$  ( $h=0.25$ ) at  $t=0, 3900$ . The vertical scale of the solution has been enlarged by a factor  $\varepsilon^{-2}$ . The lower panel represents the corresponding bottom geometry, for which  $b < 0$ .

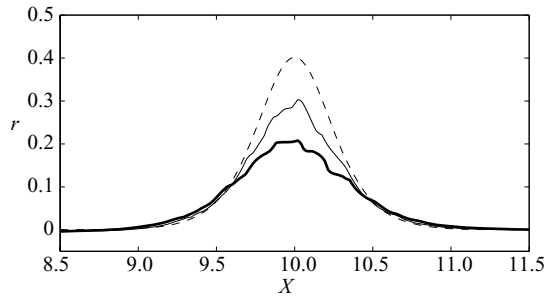


FIGURE 11. Profiles of the principal component  $r$  at  $t=0$  (dashed line), 2700 (thin solid line), 5700 (thick solid line) with the centres of mass aligned.

we remark that the scattering is not sufficient to significantly disperse solutions in the scaling regime in which we work.

Finally, we find that there is an additional mechanism that affects the growth or attenuation of solutions, which depends upon properties of skewness of the statistics

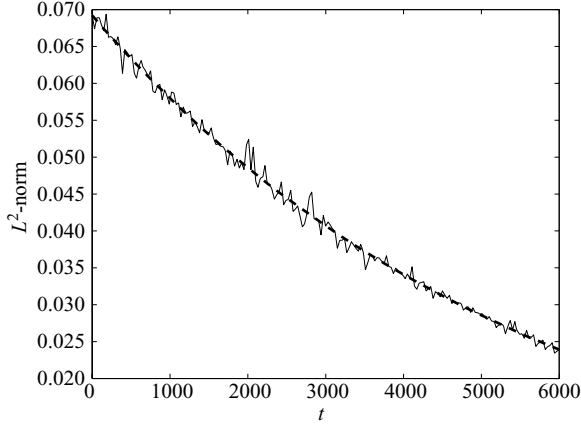


FIGURE 12. The  $L^2$ -norm of  $r$  as a function of time for  $h = 0.25$ ,  $b = -8.85 \times 10^{-3}$  and  $\varepsilon = 0.1$ , exhibiting long-time scale attenuation of the solution. The solid curve represents the numerical result, while the dashed curve represents the theoretical prediction  $e^{2be^2t} \|r^0\|_2^2$ .

of the random bottom. This is not present in the usual case of a flat bottom, and it could have the potential to be exploited in harbour design and other coastal engineering structures.

The authors are grateful to Dr O. Díaz-Espinosa for helpful discussions. W. C. was partially supported by the Canada Research Chairs Program and NSERC through grant number 238452-06. P. G. was partially supported by the University of Delaware Research Foundation and NSF through grant number DMS-0625931, and he also would like to thank the Department of Mathematics at the University of Toronto as well as the Fields Institute for their hospitality during a visit in Spring 2008. C.S. was partially supported by NSERC through grant number 46179-05.

### Appendix. Proof of two probabilistic theorems

This section contains several results in mathematical probability that are used throughout the paper.

#### *Proof of Theorem 3.1*

The space of functions  $\Omega := C^1(\mathbb{R})$ , along with a translation invariant probability measure  $\mathbf{P}$ , plays the role of the set of realizations  $\mu \in \Omega$ . With respect to translations  $\tau_y \mu(x) = \mu(x + y)$ , we assume that the probability space  $(\Omega, \mathbf{P})$  describes a stationary ergodic process. By the ergodic theorem, for every test function  $f(X)$  one has

$$\lim_{\varepsilon \rightarrow 0} \int \mu\left(\frac{X}{\varepsilon}\right) f(X) dX = \mathbf{E}(\mu) \int f(X) dX.$$

Subsequently, we may suppose that  $\mathbf{E}(\mu) = 0$  and study the asymptotic behaviour of

$$\int f(X) \mu\left(\frac{X}{\varepsilon}\right) dX = \sqrt{\varepsilon} \sigma_\mu \int f(X) \left( \frac{\sqrt{\varepsilon}}{\sigma_\mu} \partial_X \int_0^{X/\varepsilon} \mu(s) ds \right) dX + o(\sqrt{\varepsilon}).$$

We furthermore assume that the process defining  $\mu$  has mixing properties, so that by Donsker's theorem (Billingsley 1968) the quantity

$$Y_\varepsilon(\mu)(X) = \frac{\sqrt{\varepsilon}}{\sigma_\mu} \int_0^{X/\varepsilon} \mu(s) ds$$

converges weakly in law to Brownian motion  $B_\omega(X)$ . Thus we have the asymptotic result that

$$\frac{1}{\sqrt{\varepsilon}} \int f(X) \mu\left(\frac{X}{\varepsilon}\right) dX \rightarrow -\sigma_\mu \int \partial_X f(X) B_\omega(X) dX.$$

This is the essence of the statement of Theorem 3.1.

### *Proof of Theorem 5.1*

This result also follows from the ergodic theorem and Donsker's invariance principle. The set of realizations in our multiple-scale setting will be  $C(\mathbb{R}_X : C^1(\mathbb{R}_x)) = C(\mathbb{R}_X : \Omega)$ , a space of continuous functions of two variables (in fact  $C^1$  in  $x$ ). The role of the realizations is taken by functions  $\mu(x, X)$ , considered as a family of stationary ergodic processes under translations  $\tau_y \mu(x, X) = \mu(x + y, X)$ , parameterized continuously by the variables  $X$ . The multiple-scale environment of the problem is given by  $\mu = \mu(X/\varepsilon, X)$ . That is to say we consider the dependence on the first variable to be random and rapidly varying, which is then modulated by variations in the second variable. In parallel, there is a family of probability measures  $\mathbf{P}(X)$  parameterized by the modulation variable  $X$ . The family of processes  $(\mu(\cdot, X), \mathbf{P}(X))$  is assumed to be jointly stationary, ergodic for  $X \in \mathbb{R}$  and jointly mixing in the sense that for every  $f \in L^1(\mathbb{R})$

$$\left| \int f(X) [\mathbf{P}(A \cap \tau_y(B), X) - \mathbf{P}(A, X)\mathbf{P}(B, X)] dX \right| \leq \alpha(y) \|f\|_{L^1(dX)},$$

where  $\alpha(y) \rightarrow 0$  as  $|y| \rightarrow \infty$  at a sufficiently rapid rate. Furthermore the family  $\mathbf{P}(X)$  is weakly continuous in the variables  $X$ , namely that for all jointly measurable sets  $A$

$$\lim_{Y \rightarrow X} [\mathbf{P}(A, Y) - \mathbf{P}(A, X)] = 0.$$

Such multiple-scale situations may be approximated by finite sums of mixing processes over compact sets of  $X \in \mathbb{R}_X$ . Given any small  $\delta$ , we may choose a partition of unity  $\{g_m^\delta(X)\}_{m \in \mathbb{Z}}$  and a discrete set of points  $\{X_m^\delta \in \text{supp } g_m^\delta\}_{m \in \mathbb{Z}}$  such that given a realization  $\mu(x, X) \in C(\mathbb{R}_X : \Omega)$  one defines a uniform approximation to  $\mu(x, X)$  by

$$\mu^\delta(x, X) := \sum_{m \in \mathbb{Z}} g_m^\delta(X) \mu(x, X_m^\delta).$$

Consider a test function  $f(X)$ , which we assume to be smooth and of compact support. The ergodic theorem implies that

$$\lim_{\varepsilon \rightarrow 0} \int \mu^\delta\left(\frac{X}{\varepsilon}, X\right) f(X) dX = \int \sum_{m \in \mathbb{Z}} g_m^\delta(X) \mathbf{E}_{m, \delta}(\mu(\cdot, X_m^\delta)) f(X) dX.$$

Subsequently, in the limit of small  $\delta$

$$\lim_{\varepsilon \rightarrow 0} \int \mu\left(\frac{X}{\varepsilon}, X\right) f(X) dX = \int \mathbf{E}(\mu)(X) f(X) dX.$$

Subtracting the mean, we may now suppose that  $\mathbf{E}(\mu)(X) = 0$ . Using the same approximation, it suffices to consider

$$\mu^\delta\left(\frac{X}{\varepsilon}, X\right) = \sum_{m \in \mathbb{Z}} g_m(X) \mu_m^\delta\left(\frac{X}{\varepsilon}\right) = G(X)^\top M\left(\frac{X}{\varepsilon}\right),$$

which, up to terms which vanish with  $\delta \rightarrow 0$ , can also be assumed to be of mean value zero. Here  $G^\top(X) = (\dots, g_m(X), \dots)$  is the smooth partition of unity and  $M = (\dots, \mu_m^\delta : = \mu(\cdot, X_m^\delta), \dots)^\top$  is a stationary sequence of zero-mean processes with strong mixing properties. For a test function  $f(X)$  of compact support as above, only a finite number  $N$  of the processes  $\mu(\cdot, X_m^\delta)$  come into play. The limit as  $\varepsilon \rightarrow 0$  is given by Donsker's theorem

$$\begin{aligned} \lim_{\varepsilon \rightarrow 0} \frac{1}{\sqrt{\varepsilon}} \int f(X) \mu^\delta\left(\frac{X}{\varepsilon}, X\right) dX &= - \int \partial_X (f(X) G_N(X)^\top) A_N B_N(X) dX \\ &= \int f(X) G_N(X)^\top A_N \partial_X B_N(X) dX, \end{aligned}$$

where  $G_N(X)$  is a finite-dimensional vector function,  $B_N(X)$  is the standard normalized  $N$ -dimensional Brownian motion and  $A_N$  is the  $N \times N$  matrix such that  $A_N A_N^\top = \sigma_N^2$  which has entries  $(\sigma_N^2)_{ij} : = \int \mathbf{E}(\mu_i^\delta(0) \mu_j^\delta(s)) ds$ .

To identify the above limit, we calculate the covariance function of the quantity inside the integral of the right-hand side, namely

$$\begin{aligned} \rho_N(X, Y) &= \mathbf{E}(G_N^\top(X) A_N \partial_X B_N(X), G_N^\top(Y) A_N \partial_Y B_N(Y)) \\ &= \delta(X - Y) G_N^\top(X) A_N A_N^\top G_N(Y) \\ &= \delta(X - Y) \int \mathbf{E}(\mu^\delta(0, X) \mu^\delta(s, X)) ds \\ &= \delta(X - Y) \sigma_{\mu^\delta}^2(X), \end{aligned}$$

where

$$\sigma_{\mu^\delta}^2(X) = \int \mathbf{E}(\mu^\delta(0, X) \mu^\delta(s, X)) ds.$$

This uniquely characterizes processes with this covariance as being of the form

$$\sigma_{\mu^\delta}(X) dB_\omega(X).$$

Taking  $\delta \rightarrow 0$  we have thus obtained the basic result of Theorem 5.1,

$$\int f(X) \mu\left(\frac{X}{\varepsilon}, X\right) dX = \int f(X) \mathbf{E}(\mu)(X) dX + \sqrt{\varepsilon} \int f(X) \sigma_\mu(X) dB_\omega(X) + o(\sqrt{\varepsilon}).$$

This exhibits the fact that the asymptotic form of the left-hand side is defined in terms of the mean value  $\mathbf{E}(\mu)(X)$  and the diffusion process  $D(X) = \int_0^X \sigma_\mu(\theta) dB_\omega(\theta)$ .

## REFERENCES

- ARDHUIN, F. & HERBERS, T. H. C. 2002 Bragg scattering of random surface gravity waves by irregular seabed topography. *J. Fluid Mech.* **451**, 1–33.
- BAL, G. 2008 Central limits and homogenization in random media. *SIAM Multiscale Model. Simul.* **7** (2), 677–702.
- BELZONS, M., GUAZZELLI, E. & PARODI, O. 1998 Gravity waves on a rough bottom: experimental evidence of one-dimensional localization. *J. Fluid Mech.* **186**, 539–558.

- BILLINGSLEY, P. 1968 *Convergence of Probability Measures*. John Wiley.
- DE BOUARD, A., CRAIG, W., DÍAZ-ESPINOSA, O., GUYENNE, P. & SULEM, C. 2008 Long wave expansions for water waves over random topography. *Nonlinearity* **21**, 2143–2178.
- CRAIG, W., GUYENNE, P. & KALISCH, H. 2005 Hamiltonian long-wave expansions for free surfaces and interfaces. *Comm. Pure Appl. Math.* **58**, 1587–1641.
- CRAIG, W., GUYENNE, P., NICHOLLS, D. P. & SULEM, C. 2005 Hamiltonian long-wave expansions for water waves over a rough bottom. *Proc. R. Soc. Lond. A* **461**, 839–873.
- CRAIG, W. & SULEM, C. 2009 Asymptotics of surface waves over random bathymetry *Quart. J. Appl. Math.* (in press).
- DEVILLARD, P., DUNLOP, F. & SOUILLARD, B. 1988 Localization of gravity waves on a channel with random bottom. *J. Fluid Mech.* **186**, 521–538.
- DEVILLARD, P. & SOUILLARD, B. 1986 Polynomially decaying transmission for the nonlinear Schrödinger equation in a random medium. *J. Stat. Phys.* **43**, 423–439.
- FOUQUE, J.-P., GARNIER, J. & NACHBIN, A. 2004 Time reversal for dispersive waves in random media. *SIAM J. Appl. Math.* **64** (5), 1810–1838.
- GARNIER, J., MUÑOZ GRAJALES, J. C. & NACHBIN, A. 2007 Effective behaviour of solitary waves over random topography. *Multiscale Model. Simul.* **6**, 995–1025.
- GRATALOUP, G. & MEI, C. C. 2003 Long waves in shallow water over a random seabed. *Phys. Rev. E* **68**, 026314.
- VAN GROESEN, E. & PUDJAPRASETYA, S. R. 1993 Uni-directional waves over slowly varying bottom. Part I. Derivation of KdV type equation. *Wave Mot.* **18**, 345–370.
- HOWE, M. S. 1971 On wave scattering by random inhomogeneities, with application to the theory of weak bores. *J. Fluid. Mech.* **45**, 785–804.
- MEI, C. C. & HANCOCK, M. 2003 Weakly nonlinear surface waves over a random seabed. *J. Fluid Mech.* **475**, 247–268.
- MEI, C. C. & LI, Y. 2004 Evolution of solitons over a randomly rough seabed. *Phys. Rev. E* **70**, 016302.
- NACHBIN, A. 1995 The localization length of randomly scattered water waves. *J. Fluid Mech.* **296**, 353–372.
- NACHBIN, A. & SØLNA, K. 2003 Apparent diffusion due to topographic microstructure in shallow waters. *Phys. Fluids* **15**, 66–77.
- NAKOULIMA, O., ZAHIBO, N., PELINOVSKY, E., TALIPOVA, T. & KURKIN, A. 2005 Solitary wave dynamics in shallow water over periodic topography. *Chaos* **15**, 037107.
- PIHL, J. H., MEI, C. C. & HANCOCK, M. 2002 Surface gravity waves over a two-dimensional random seabed. *Phys. Rev. E* **66**, 016611.
- ROSALES, R. & PAPANICOLAOU, G. 1983 Gravity waves in a channel with a rough bottom. *Stud. Appl. Math.* **68**, 89–102.
- ZAKHAROV, V. E. 1968 Stability of periodic waves of finite amplitude on the surface of a deep fluid. *J. Appl. Mech. Tech. Phys.* **9**, 190–194.